ELSEVIER

Journal of Alloys and Compounds 444–445 (2007) 177–183

Journal of ALLOYS AND COMPOUNDS

www.elsevier.com/locate/jallcom

Heat treatment effects on the surface chemisorption behavior of strained uranium: The H_2O/U reaction

E. Tiferet [a], M.H. Mintz [a,b], S. Zalkind [b], I. Jacob [a], N. Shamir [b,*]

[a] *Department of Nuclear Engineering, Ben-Gurion University of the Negev, POB 653, Beer-Sheva 84104, Israel*
[b] *Nuclear Research Centre-Negev, POB 9001, Beer-Sheva 84190, Israel*

Received 31 July 2006; received in revised form 24 October 2006; accepted 26 October 2006
Available online 28 November 2006

Abstract

The initial interaction of H_2O vapor with polycrystalline uranium surfaces was studied with samples initially strained, then strain relieved by heat treatments, performed in the temperature range up to ~650 K. The chemisorption characteristics of these surfaces were studied by a combination of direct recoils spectrometry and X-ray photoelectron spectroscopy. X-ray diffraction measurements were used to determine the level of strain relief induced by each of the heat treatments. For all the samples, full water dissociation on the metal surface is observed. The reactivity of the samples towards water is clearly strain dependent, with the sticking coefficient decreasing as strain is relieved. It also seems that for strained samples the initial growth of the oxide is mostly inwards, while for the more relaxed samples lateral growth is dominant. Two interesting phenomena were observed for specific samples. For the 420 K relieved sample, partial dissociation process is observed on top of the forming oxide, in contrast to the full dissociation observed for the other samples. For the ~650 K relieved sample, clustering of the adsorbed hydrogen atoms (resulted by water dissociation) on the metal surface is observed, in contrast to the homogeneous dispersion of H, occurring on the surface of all other samples. These two phenomena will further be studied in conjunction with microscopic metallurgical observations.

Keywords: Actinide alloys and compounds; Gas–solid reactions; Oxidation; Ion impact; Photoelectron spectroscopies

1. Introduction

Understanding the interactions of water vapor and metallic surfaces is an important issue due to its relation to environmental corrosion processes. Yet, studies on the very initial steps of these interactions, especially at ambient temperatures, are not adequately completed to the extent that the complex mechanisms, controlling these reactions, are conclusively elucidated [1,2]. It is commonly accepted that most of the transition metals tend to dissociate the chemisorbed water at room temperature [1]. The dissociation may be complete (i.e. into 2H + O), partial (i.e. into H + OH) or a combination of these two possibilities. Hence, a mixture of H, O and OH entities is generally anticipated to accumulate on metallic surfaces exposed to water. However, very few direct observations of these species and their kinetic behavior have been reported. One of the difficulties encountered in the studies of the interaction of water with metallic surfaces is the direct detection of hydrogen or hydrogen containing species, such as hydroxyl groups. For the latter, indirect probing such as chemical shifts in the accompanying O(1s) X-ray photoelectron spectroscopy (XPS) peaks [1], photon-stimulated desorption (PSD) or electron-stimulated desorption (ESD) [3,4] are sometimes used. However, such determinations are not conclusive and may be interpreted in different ways [1,2]. Other techniques, which in principle are sensitive to the presence of hydrogen atoms on the surface, utilized in some of these studies are secondary ion mass spectrometry (SIMS) and temperature programmed desorption (TPD). Still, as pointed out before [5,6], hydrogen signal intensities measured by most SIMS set-ups are strongly affected by the respective ion yield fractions, which turn to be sensitive to the chemical matrix effects. Hence the interpretation of such signal intensity variations is complicated by the convolution of two simultaneous factors, namely, surface concentrations and the above mentioned chemical matrix effects. The interpretation of TPD results is also somewhat ambiguous due to recombination effects (especially for hydrogen) on the surface and the inability, sometimes to distinguish between surface and subsurface products.

* Corresponding author. Tel.: +972 8 6568785; fax: +972 8 6568751.
E-mail address: noah.shamir@gmail.com (N. Shamir).

0925-8388/$ – see front matter © 2006 Elsevier B.V. All rights reserved.
doi:10.1016/j.jallcom.2006.10.103

A complementary powerful technique for such studies is the direct recoils spectrometry (DRS) previously reviewed [6,7]. This method is insensitive to ion-fractions, hence to chemical matrix effects changes, which enables the decoupling between chemical and concentration parameters. Also, unlike SIMS or electron spectroscopy methods, DRS can probe different atomic geometrical arrangements on the surface (due to its sensitivity to shadowing/blocking effects [5,6]). This capability can be used to elucidate geometry related phenomena associated with the surface chemisorption process. Thus, for example, it has been utilized in the study of the H_2O/Ti system [2] to resolve between two parallel chemisorption routs—a direct-collision (Langmuir type) that yields isolated, perpendicular to the surface OH species, and a precursor state route yielding clusters of tilted OH moieties.

For the system H_2O/U, two studies, using the combination of DRS and electron spectroscopy, were lately performed by our group. The first study [8], was performed on a strained sample, slightly relieved (hence labeled Sample B) and the second one [9] on a more strain relieved sample (hence Sample C), revealing different mechanisms of adsorptions. In addition, SIMS, XPS, Auger electron spectroscopy (AES), ultra-violet photoelectron spectroscopy (UPS) and TPD were applied before, to the study of the water–uranium reaction [10–12]. The reaction of water with UO_2 was also studied [13–16], using, besides the above techniques, also ESD, low energy electron diffraction (LEED) and low energy ion scattering (LEIS). Winer et al. [10] proposed fast oxidation and strongly bound OH^- species on the formed oxide. Balooch and Hamza [11], on one hand, attributed low temperature desorption of H_2 in the TPD measurements to hydrogen adsorbed on top of the formed oxide. Stultz et al. [15] and Senanayake and Idriss [16] also claimed the same about hydrogen adsorbed on defects on UO_2(1 0 0) and UO_2(1 1 1) surfaces respectively. Manner et al. [12], on the other hand, performed a careful study of H_2 desorption versus surface coverage and claimed that hydrogen resides only on non-oxygen (or oxide) covered patches of the uranium surface and H_2 desorption from a totally covered (non-defective) surface stems from subsurface hydrogen.

It is known that the recrystallization process in uranium starts at approximately 600–700 K [17], while lower temperature annealing results in only recovery [17], meaning that the number of the dislocations are not reduced nor their density. Nevertheless, a rearrangement of the dislocations decreases the stress. Heating to higher temperatures and cooling causes grain growth and inflicts thermal strain due to the anisotropy of thermal expansion of uranium [18,19].

The present study concentrates on the effect of strain and its thermal relief on the surface processes and mechanisms. The main goal of the study was to try to correlate the surface processes to the bulk defects (dislocations) resulting from strain, inflicted on the samples and their cure by annealing. The current article summarizes the previous results published on this system [8,9], adds a large amount of new observations and presents an up-to-date whole picture the surface processes of the various heat treated samples and their correlations to the strain relief.

2. Experimental

2.1. The experimental system

An ultra-high-vacuum (UHV) chamber ($\sim 2 \times 10^{-10}$ Torr baseline pressure) incorporated with XPS and DRS [5–7], was used in the present study. The DRS technique is extremely surface-sensitive, probing the topmost atomic layer of the solid. Hence, combined measurements with electron spectroscopy methods (e.g. AES, XPS, etc.) may resolve between processes taking place on the outermost surface layer and those occurring at the subsurface region [20,21]. Due to the grazing angle used, geometrical information may be gained from the effects of shadowing of hydrogen atoms by neighboring larger ones.

2.2. Experimental procedures

Polycrystalline samples of strained (formed by hot worked rolling) uranium, treated thermally to partially or fully relieve the strain, were used in this study.

The samples were mechanically polished down to 1 μm smoothness, using diamond paste, leading to a mirror like surface, cleaned in distilled water, acetone and ethanol. One sample was studied as received (AR), and the others were heated, in the UHV system, to 420 K, 520 K or ∼650 K for 48 h to relieve the strain. The samples will be named henceforth A for the not treated sample, and B, C and D, for the 420 K, 520 K and ∼650 K treated samples, respectively.

The samples were scanned using an optical microscope and SEM (showing grains of ten micrometers size, not presented). XRD was performed on all of them.

In the UHV system, sputter cleaning was performed by a rastered, differentially pumped ion gun, using 5 keV Ar^+ ions, with a current of about 5 μA/cm^2. Sputtering was carried long enough, so the former stressed bulk will be reached. Distilled water contained in a stainless steel reactor was used after a few freeze–pump-thaw cycles in order to reduce the gases dissolves in the water, and the water (or oxygen) pressure in the chamber was controlled by a leak valve. The water cleanliness during exposure was monitored by residual gas analysis. The DRS measurements were performed with continuous exposure to water vapor during the measurement, while the XPS runs were performed following fixed doses of exposure. All exposures were performed by backfilling the UHV chamber with gas, measuring the pressure with a Bayard–Alpert gauge and regulating the H_2O stability with a mass-spectrometer.

All exposures and measurements, presented in the present study, were performed at room temperature (RT).

3. Results

XRD measurements performed on all the samples yielded different preferred orientations and line widths. For the [0 0 2] line, the widths are A: 0.35°, B: 0.23°, C and D: 0.17°.

Fig. 1A–D presents O(DR) and H(DR) exposure curves and Fig. 2 depicts the H(DR)/O(DR) ratio versus the exposure dose (expressed in Langmuirs, 1 L = 10^{-6} Torr × s) for all samples. In all graphs the O(DR) intensity was normalized so that the saturation value attains unity, while that of H(DR) scales to the normalized O(DR). For all samples except D (∼650 K treatment), the H(DR) initially increases with increasing exposure dose, reaching a local maximum value at a very low exposure, then decreasing with further exposure, attaining a minimum followed by an intensity increases reaching finally a saturation value.

The chemical nature of the water–uranium reaction products can be partially obtained from the XPS measurements. Two regions of the spectrum are of interest in this study: the O 1s core level of the oxygen and the U 4f core level of the uranium peaks. Figs. 3 and 4 display the O 1s and U 4f, respectively, XPS measurements for Sample B for various exposures. In addition

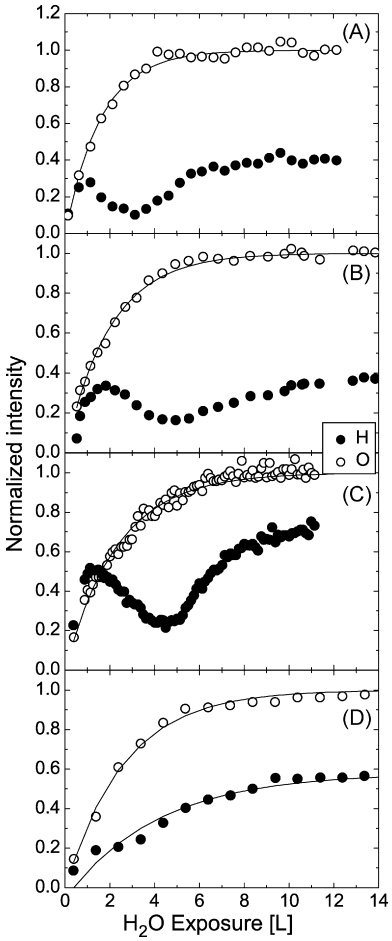

Fig. 1. O(DR) and H(DR) vs. H_2O exposure for all the studied samples. The saturation value of O(DR) is normalized to 1 (full coverage). Clustering mechanism fits are displayed for the O(DR) curves and for the Sample D H(DR).

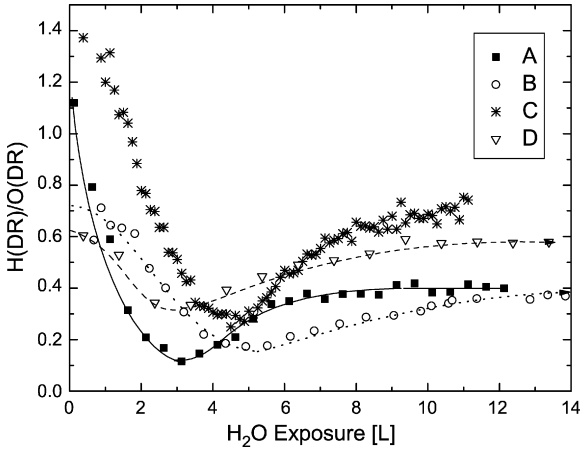

Fig. 2. H(DR)/O(DR) vs. H_2O exposure for all the samples. The lines are just guides to the eye.

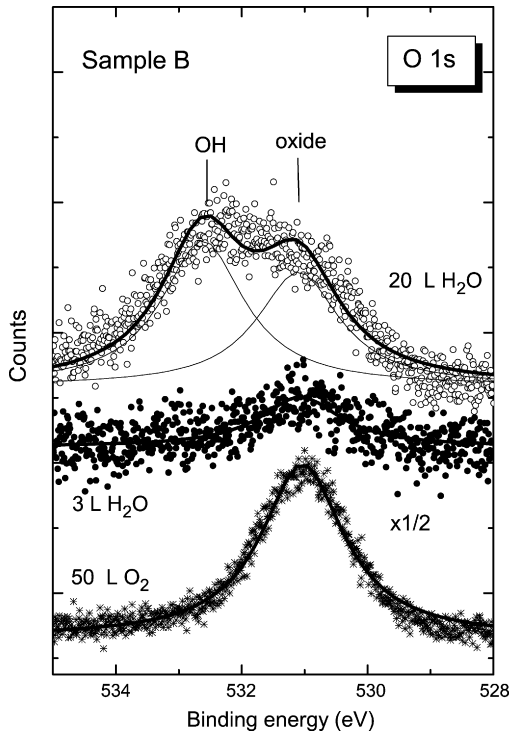

Fig. 3. Sample B: XPS O 1s line for 3 L and 20 L water vapor exposure together with that of 50 L O_2 exposure. Lorenzian fits for oxidic and OH contributions are plotted. The parameters of the oxidic contribution were fixed in the water exposure fits to those obtained for the O_2 one.

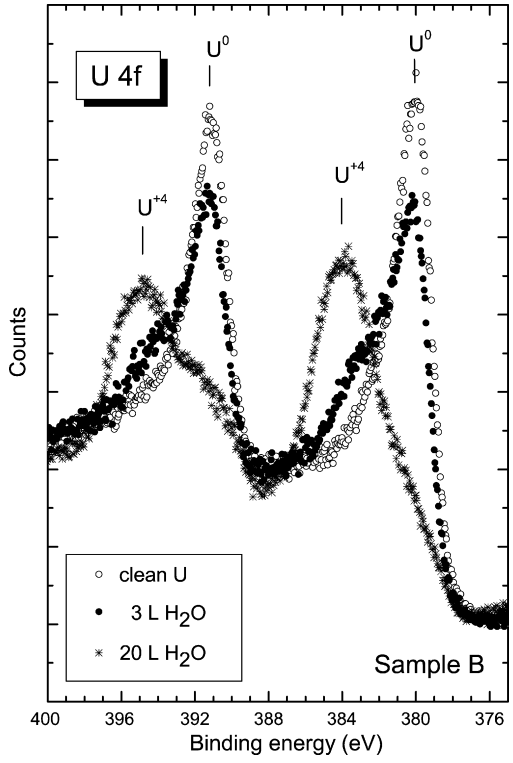

Fig. 4. Sample B: XPS U 4f lines for clean uranium and 3 L and 20 L water vapor exposures. The energies of metallic uranium (0) and +4 uranium are indicated.

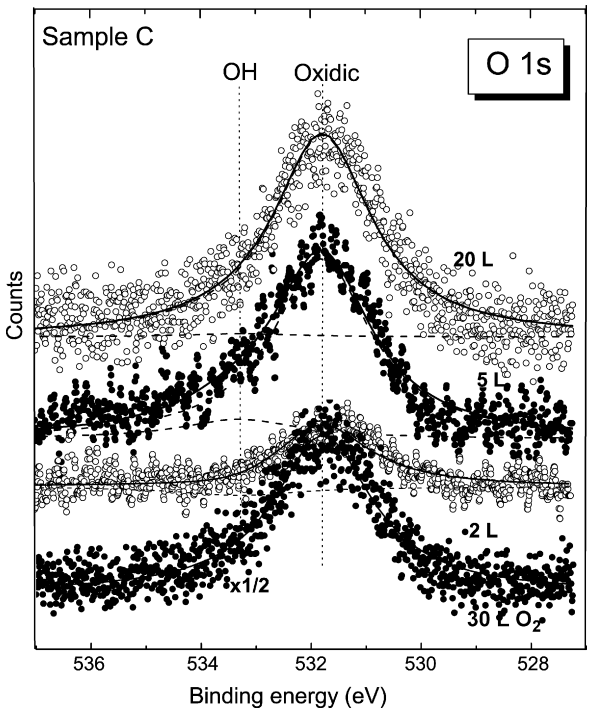

Fig. 5. Sample C: XPS O 1s line for 5 L, 10 L and 40 L water vapor exposure together with that of 30 L O_2. Lorenzian fits were performed by the same procedure as for Sample B.

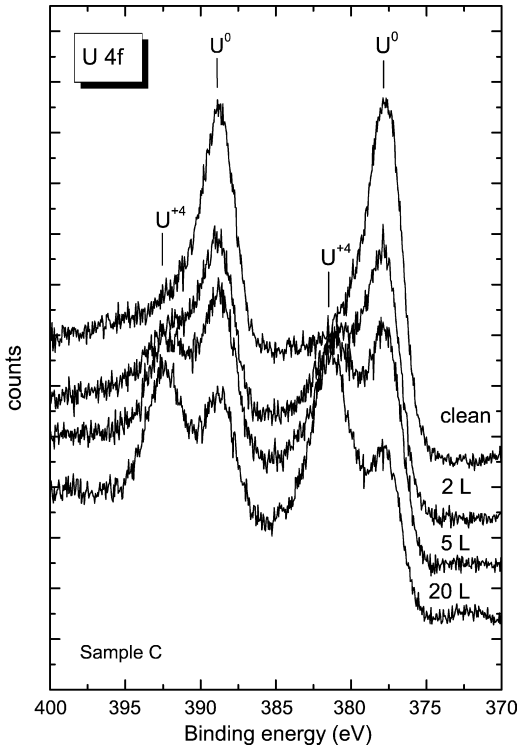

Fig. 6. Sample C: XPS U 4f lines for clean uranium and 5 L, 10 L and 40 L water vapor exposures. The energies of metallic uranium (0) and +4 uranium are indicated.

to the oxidic oxygen (at 531 eV), there is a strong contribution shifted about 1.5 eV to a higher binding energy, typical to hydroxylic oxygen. Figs. 5 and 6 display the same spectra for Sample C and it is clearly seen that the hydroxylic contribution is not present. For the Samples A and D, the O 1s spectra, taken prior to H(DR) minimum, at the minimum and at saturation (not presented) are similar to those of Sample C (at the same exposure doses), namely, only oxidic oxygen is present.

4. Discussion

4.1. The shadowing model

The shadowing model was presented in previous publications [8,9]. Essentially, it makes use of shadowing of surface hydrogens by neighboring oxygen atoms, while hydrogens sitting on top of oxygens (OH) are not shadowed. This enables the distinction between partial ($H_2O \rightarrow OH + H$) and full dissociation ($H_2O \rightarrow O + 2H$).

Partial dissociation yields an attenuation factor of 2 between the initial coverage H(DR)/O(DR) ratio to the final one. For full dissociation, the attenuation factor is infinity. An attenuation factor between 2 and infinity, points to a mixture of the full and partial dissociation routes.

4.2. Oxygen and hydrogen accumulation

O(DR) indicates the surface coverage with oxygen, that can be in the form of adsorbed oxygen or OH and in a certain stage transform into an oxide. H(DR)/O(DR) together with the O 1s XPS spectrum determines the surface state of adsorbed oxygen, while the U 4f spectrum depicts the appearance of the U^{+4} peak, associated with oxide formation (UO_2). For all samples, O(DR) was successfully fitted to the clustering model [22] rather than to the double site one (not shown).

The DRS curves for all samples (Fig. 1A–E), which are discussed in detail below, indicate hydrogen continuous accumulation on the surface. Part of this hydrogen seems to be associated with hydroxyls only for Sample B, as indicated by the XPS O 1s spectrum (Fig. 3).

4.3. The specific samples

4.3.1. Sample A, no stress relief

For 4 L H_2O exposure, O(DR) reaches saturation (Fig. 1A), completing the outermost layer (hence normalized to 1). XPS O 1s (not presented) shows a single peak at the oxidic oxygen energy, which suggests full dissociation. The decrease of the H(DR)/O(DR) ratio (Fig. 2) from its initial value to a minimum, with a relatively large attenuation factor (∼10), clearly indicates full dissociation.

Upon further oxidation, the H/O ratio increases, probably due to hydrogen accumulation on the formed oxide (which starts to form prior to full coverage of the surface, hence the H/O ratio does not go all the way to zero due to full shadowing), not bound to an oxygen atom (still single O 1s oxidic peak).

The U 4f core levels peaks (not presented) show an attenuation of the metal peak along with buildup of the oxide peak as expected.

Table 1
DRS saturation and minimum dose values and saturation relative H(DR) value

Type (recovery temperature)	O(DR) saturation value (L)	H(DR) minimum value (L)	H(DR) saturation value (L)	H(DR) minimum relative intensity	H(DR) saturation relative intensity	Calc. oxide thickness at about twice O saturation)
A (AR)	4	3	8	0.09	0.60	12
B (420 K)	5.5	4.5	13	0.17	0.39	9
C (520 K)	8	4.5	10	0.24	0.72	8
D (∼650 K)	9	none	9	none	0.56	9

The oxide thickness is given in Angstoms.

4.3.2. Sample B, 420 K recovery

The initial interaction of water vapor with Sample B was presented in a previous publication [8] in detail. Full dissociation occurs on the clean metal but on the oxide the partial dissociation takes place (Fig. 3). The formation of oxide starts at a low exposure (3 L H_2O, Fig. 4). This accounts, again, for the fact that the minimum of H(DR) is not going to zero (as OH starts to form on the oxide).

4.3.3. Sample C, 520 K recovery

The study of this sample was also presented in detail in a previous publication [9]. Here again, as in Sample A, full dissociation is dominant on both the metal and on the oxide as well (Fig. 5). It is assumed that a two-step-dissociation takes place: initially water molecules dissociate, on the oxide, into OH^- and H^+, the H^+ being neutralized by an electron tunneling from the metal and resides on the oxide surface (not bound to oxygen as a hydroxyl). The OH^- diffuses by a Mot-Cabrera mechanism into the metal oxide interface and dissociates into H and O^{-2} without influencing the DRS spectra that is sensitive only to the surface species. Here too, the initial growth of oxide starts as early as for 5 L H_2O exposure (Fig. 6).

4.3.4. Sample D, ∼650 K recovery-recrystallization

At this temperature of heating the sample, recrystallization occurs [17]. XPS O 1s (not presented) shows full dissociation for the full exposure range. The U 4f spectrum (not presented) indicates early oxidation, similar to the other samples.

Fig. 1D presents an unusual monotonous increase of H(DR) versus exposure, similar to that of O(DR), with a minor shadowing effect. Clustering best fit for H(DR) yielded $s_0 \sim 0.15$ for H(DR) (the small shadowing present, somewhat lowers the calculated value). H atoms seem to cluster instead of randomly disperse like for the other (A–C) samples, with similar conditions. Some shadowing barely occurs, probably at the border of the oxygen and hydrogen clusters. It seems that for all other samples, hydrogen can adsorb on a different set of sites than oxygen (in addition, maybe, to the oxygen sites), allowing it a uniform spread, including inside oxygen clusters areas, hence the efficient shadowing. It seems that the recrystallization caused a closure of this set of sites, sending the hydrogen atoms to compete with oxygen on the adsorption sites, which explains the low s_0(H) value. Alternatively, an O–H repulsion developing on the surface (which may be caused by an electronic effect due to the changing conditions caused by the re-crystallization) can prevent a mixture of the two species, even if close adsorption sites are available. An example of such repulsion on the surface between oxygen and hydrogen specifically has been observed before [23] as well as other surface repulsion phenomena between species that usually attract each other [24]. Alternative explanations that can not be ruled out are an initial subsurface migration of adsorbed hydrogen atoms and only a later surface accumulation (that will "flatten" the initial increase and decrease towards a minimum of the H(DR) curve), or adsorption of tilted OH clusters on the metal surface, so the hydrogen is shadowed and the OH shift is not observed by XPS [2].

4.4. Comparison

For the entire studied samples, water adsorption on the metal surface results in full dissociation of the water molecule. For all of them, except for Sample B, also on to of the formed oxide, the dissociation of water is full.

The average thickness of the forming oxide can be calculated for the decrease of the metallic (U^0) peak in the U 4f spectra, as well as from the increase of the oxidic peak (U^{+4}). The calculations performed yielded similar results for all samples, except for B, where the U^0 decrease stems also from the OH coverage on top of the oxide.

Table 1 summarizes the various O(DR) and H(DR) parameters, presented in Fig. 2, with the addition of the calculated oxide thickness, measured for all the samples at about twice the saturation exposure for the O(DR) line. All values are similar, except for the higher value for A, the most strained sample, which is supposed to be most reactive.

Comparing the O(DR) saturation values to those of H(DR) minimum, one can see that for the more strained Samples A and B, the H(DR) minimum is close to the O(DR) saturation, indicating a relatively late buildup of oxide coverage on the surface (and OH or H on top), so the shadowing of surface hydrogen by neighboring adsorbed oxygen is most effective towards full coverage. For Sample C, where the U 4f spectrum (Fig. 6) indicates not significantly less oxide buildup at the H(DR) minimum, the O(DR) saturation exposure is significantly higher, indicating lateral rather then in-depth growth (so more surface is covered by the same amount of oxide). Early significant coverage by oxide shifts the H(DR) minimum to the pre-oxide stage (efficient shadowing). For all the samples, non-shadowed hydrogen is present only on top of the oxide (for B, in hydroxyls), so the saturation of H(DR) indicates the closure of an oxide layer. For the more strained samples (A, B), because of the in depth growth, the closure of oxide layer is relatively late compared to O(DR)

Table 2
Initial sticking coefficients, s_0(O) and s_0(H), for Samples A–D

	s_0(O)	s_0(H)
A (AR)	1	0.5
B (420 K)	0.8	0.4
C (520 K)	0.7	0.4
D (~650 K)	0.6	>0.15[a]

[a] The small shadowing present, somewhat lowers the calculated value.

saturation, so the oxygen layer is first closed by mostly adsorbed oxygen. For the more relaxed samples (C, D), the H(DR) saturation is close to that of the O(DR) one, due to the lateral growth of the oxide that dominates the surface coverage upon closure of the oxygen layer.

Table 2 presents the initial sticking coefficients for oxygen and hydrogen, s_0(O) and s_0(H), respectively, for Samples A–D. For Sample A (supposed to be the most reactive, having most defects) s_0 was assumed to be 1, as found in a previous study [10], the fit yielded the reasonable value of $N_{max} = 5.8 \times 10^{15}$ sites/cm^2 (s_0 is the initial sticking coefficient; N_{max} is the maximal number of atomic or molecular adsorption sites on a cm^2 of the surface,). The s_0 for the other samples were calculated using this value of N_{max}. s_0 for hydrogen was calculated from the H(DR) relative slope (compared to oxygen), taking into account two hydrogen atoms per oxygen and the same N_{max} (although it may be different for hydrogen). Since the initial slope is less well determined, when a model is not involved, s_0(H) for all samples except D (where it was calculated from the fit to the clustering model) values are more of an estimate.

It is quite clear that recovery of stressed metal influences the surface reactivity that is a manifestation of the bulk one. As mentioned before, the full dissociation on the oxide seems to be a two-step process (partial dissociation and then migration of the hydroxyls to the metal/oxide interface and further oxidation). Two different mechanisms seem to take place: the first one is the enhancement of full dissociation due to more defects on the surface of stressed uranium, as seen from the high s_0(O) for Sample A, decreasing gradually with stress relief. The other mechanism seems to be a non-monotonous one, namely the formation of specific defects on the oxide formed on Sample B (due to surface defects on the metal) that strongly bind the OH, formed by the first step of dissociation.

Fig. 7 presents H(DR)/O(DR) versus O(DR) (surface coverage by oxygen species), for all the samples. This presentation enables comparative observation of the process as function of surface coverage that has more common parameters, for all samples, than exposure. For all samples, it is clear that on the metal, the H/O decreases with the increase of coverage (due to full dissociation), with the increase of shadowing efficiency. For D, shadowing is minimal (probably at mutual cluster edges), hence the small gradient of H/O versus coverage. For the more strained samples (A, B) the minimum is deeper and comes at a later coverage, probably due to less oxide coverage, compared to C and D. For all the samples, the increase, following most efficient shadowing at the minimum, is due to hydrogen accumulation on top of the formed oxide, as H atoms residing on the surface, as

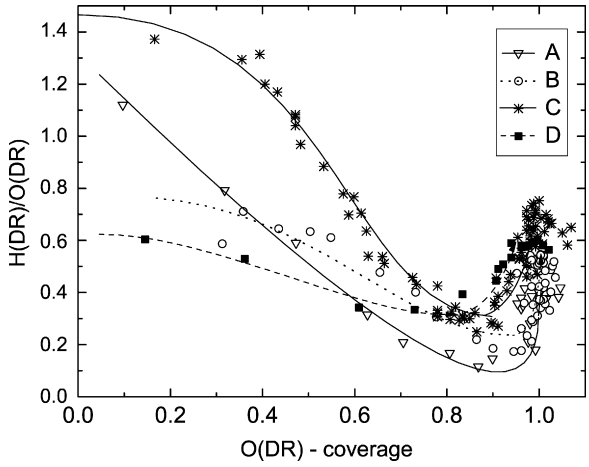

Fig. 7. H(DR)/O(DR) vs. oxygen coverage, O(DR) (taken from Fig. 1), for all the samples. The lines are just guides to the eye.

is the case for all samples, except for B where the accumulation is of OH.

4.5. The effect of strain and its relief on the surface processes

Rolling and the strain it causes, mostly form dislocations in the bulk that are present also on the surface (that has been revealed by sputtering). From our experience [25], the sputtering itself does not change the surface mechanisms, and only enhances its reactivity. This aspect will be covered, however, by a comparative study of a sputtered versus annealed surface that will be performed on Sample D (the only one that will not change by annealing).

Some of the adsorption and oxidation parameters that were measured in this study seem to be directly influenced by stress and its relief:

(a) Reactivity, as manifested by the initial sticking coefficient s_0: Fig. 8 presents the XRD linewidth for the differently treated samples, together with s_0(O). The correlation is

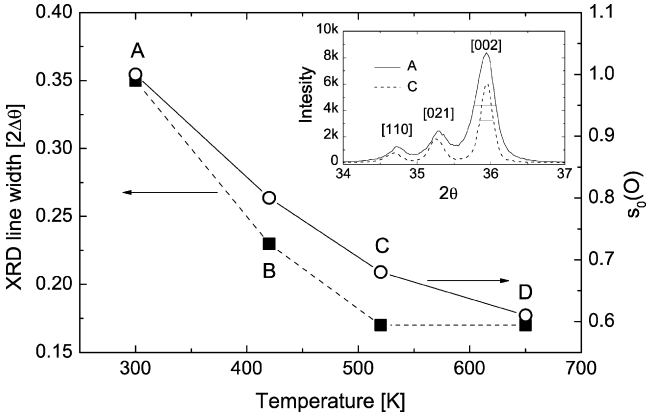

Fig. 8. XRD [0 0 2] linewidth (left axis) and the initial oxygen sticking coefficient, s_0(O) (right axis) for the four samples. Inset: partial XRD spectrum for Samples A and C. The linewidth at half height is indicated.

clear. For Sample D, no additional strain relief is observed, in comparison to C, but it seems that the recrystallization (movement of dislocations to the new grain boundaries) added to the decrease in reactivity.

(b) Initial oxidation: it seems that the more strained Samples A and B oxidize more inwards than laterally, where strain related defects are probably the easy inward channels of oxidation, so the oxide coverage is not significant when the first layer is fully covered by oxygen. For the more relaxed Samples C and D, the oxide grows mostly laterally, so the closure of the first oxygen covered layer is mostly oxide coalescence.

Other parameters are clearly different for the different samples, but cannot be correlated to a specific relaxation process:

(a) Partial versus full dissociation on top of the forming oxide: Sample B, which is slightly relaxed, is the only sample that presented a clear buildup of hydroxyls on to of the formed oxide layer with continuous exposure to water vapor, in contrast to all other samples studied, where full dissociation occurs on top of the oxide.

(b) In contrast to all other samples, where clustering occurs for oxygen, and the hydrogen (resulted by water dissociation) homogeneously disperses on the metal surface, for Sample D, clustering seems to occur also for hydrogen with no mixing between the clusters of the two species.

5. Summary and conclusions

The following facts were established in the present study:

1. On all samples, AR as well as heat-treated ones, full dissociation of water molecules was observed on the metal surface. On the forming oxide, full dissociation was observed for Samples A, C, D and partial dissociation on B.
2. Clustering adsorption of oxygen (from the dissociation products) was observed on all the samples. Homogeneous dispersion of hydrogen was observed on Samples A–C, while for Sample D the adsorption was of a clustering nature.
3. Oxidation of all samples, started before the closure of the first adsorbed layer. For the more strained Samples A and B, the growth is mostly inwards, probably due to defects. The more relaxed Samples C and D, the oxide grows mostly laterally.
4. The sticking coefficient for oxygen, indicating the reactivity of the sample, decreases the more annealing is applied. This correlates well with the reduction of the number of bulk defects (that are manifested on the surface).

The main task of the present study was to correlate stress, inflicted on uranium by hot work rolling and its relief by heat treatment, to the parameters of water adsorption and oxidation. It is evident that the differently treated samples present different parameters of adsorption and oxidation as can especially be observed in Fig. 1. Some of these parameters can be directly correlated to stress and its relief, as discussed in the previous section and some seem to be anomalies, special to a certain state of the surface, formed by the stress and the specific treatment it underwent, without being able (at this stage), to correlate the phenomena observed to any specific parameters.

It is clear, at this stage, that XRD linewidth and optical metallurgical micrographs are not enough to determine the surface state, so full understanding of the processes can be achieved. A microscopic observation of the bulk structure is needed in order to better understand the parameters that determine the processes. It is also clear that in order to determine the contribution of surface sputtering to the processes, a comparative study of sputtered versus annealed surface is needed and it is the intention to carry it out.

Again, it was demonstrated that DRS, and particularly the shadowing model that is especially effective for water dissociation, in association with electron spectroscopy methods (XPS, in the present case) serves as a powerful tool for studying surface structures and processes.

Acknowledgments

This work was partially supported by grants from the Israel Council for Higher Education and the Israel Atomic Energy Commission and the Ministry of National Infrastructure, Division of R&D. The authors wish to thank G. Kimmel for a fruitful discussion.

References

[1] P.A. Thiel, T.E. Madey, Surf. Sci. Rep. 7 (1987) 211;
M.A. Henderson, Surf. Sci. Rep. 46 (2002) 1.
[2] A. Azoulay, N. Shamir, V. Voltera, M.H. Mintz, Surf. Sci. 422 (1999) 141.
[3] R. Stockbauer, D.M. Hanson, S.A. Flodstrom, T.E. Madey, Phys. Rev. B 26 (1982) 1885.
[4] G. Strasser, G. Rosina, E. Bertel, F.P. Netzer, Surf. Sci. 152/153 (1985) 756.
[5] M.H. Mintz, J.A. Schultz, J. Less-Common Met. 103 (1984) 349.
[6] J.W. Rabalais, CRC Crit. Rev. Solid State Mater. Sci. 14 (1988) 318.
[7] M.S. Hammond, J.A. Schultz, A.R. Krauss, J. Vac. Sci. Technol. A 13 (1995) 1136.
[8] M.H. Mintz, N. Shamir, Appl. Surf. Sci. 252 (2005) 633.
[9] N. Shamir, E. Tiferet, S. Zalkind, M.H. Mintz, Surf. Sci. 600 (2006) 657.
[10] K. Winer, C.A. Colmenares, R.L. Smith, F. Wooten, Surf. Sci. 183 (1987) 349.
[11] M. Balooch, A.V. Hamza, J. Nucl. Mater. 230 (1996) 259.
[12] W.L. Manner, J.A. Lloyd, M.T. Paffett, J. Nucl. Mater. 275 (1999) 37.
[13] M.N. Hedhili, B.V. Yashinskiy, T.E. Madey, Surf. Sci. 445 (2000) 512.
[14] M.T. Paffett, D. Kelly, S.A. Joyce, J. Morris, K. Veirs, J. Nucl. Mater. 332 (2003) 45.
[15] J. Stultz, M.T. Paffett, S.A. Joyce, J. Chem. Phys. B 108 (2004) 2362.
[16] S.D. Senanayake, H. Idriss, Surf. Sci. 563 (2004) 135.
[17] D.R. Askeland, The Science and Engineering of Metals, PWS Publishing comp, Boston University of Missouri-Rolla, 1994, p. 190.
[18] E. Tiferet, N. Shamir, unpublished results.
[19] G. Kimmel, private communication.
[20] E. Swissa, J. Bloch, U. Atzmony, M.H. Mintz, Surf. Sci. 214 (1989) 323.
[21] E. Swissa, I. Jacob, U. Atzmony, N. Shamir, M.H. Mintz, Surf. Sci. 223 (1989) 607.
[22] D.A. King, M.G. Wells, Proc. R. Soc. Lond. A 339 (1975) 245.
[23] S. Zalkind, M. Polak, N. Shamir, Surf. Sci. 539 (2003) 81.
[24] J.C. Lin, N. Shamir, R. Gomer, Surf. Sci. 206 (1988) 61;
N. Shamir, J.C. Lin, R. Gomer, Surf. Sci. 214 (1989) 74;
N. Shamir, R. Gomer, Surf. Sci. 216 (1989) 49.
[25] S. Zalkind, M. Polak, N. Shamir, Surf. Sci. 513 (2002) 501.